Mon. Not. R. Astron. Soc. **365,** 1235–1242 (2006) doi:10.1111/j.1365-2966.2005.09813.x

Model of optical turbulence profile at Cerro Pachón

A. Tokovinin[1]★ and T. Travouillon[2]★

[1]*Cerro-Tololo Inter American Observatory, Casilla 603, La Serena, Chile*
[2]*California Institute of Technology, 1200 E. Californias Blvd, Pasadena, CA 91125, USA*

Accepted 2005 October 28. Received 2005 October 26; in original form 2005 May 26

ABSTRACT

New measurements of optical turbulence profile at the Cerro Pachón observatory in Chile are analysed jointly with previously published data to model the variations of the intensity and thickness of the ground layer and free atmosphere under a variety of observing conditions. This work is motivated by the need to predict statistically the performance of ground-layer adaptice optics. We find that the ground-layer profile can be represented by a decaying exponent with a scale height of 20–40 m, increasing to 100 m under bad conditions. The zone from 6 to 500 m contributes typically about 61 per cent to the total integral, the latter causing a median seeing of 0.77 arcsec. Turbulence integrals in the ground layer and in free atmosphere vary independently of each other, in 50 per cent of cases they deviate by less than 1.8 times from their respective median values. The existence of periods with low turbulence in the free atmosphere and their importance for adaptive optics is stressed.

Key words: atmospheric effects – instrumentation: adaptive optics – site testing.

1 INTRODUCTION

The Cerro Pachón (CP) mountain in Chile (2738 m a.s.l., 70°44′01″W, 30°14′17″S) hosts the 8-m Gemini-South telescope and 4-m SOAR telescope. Both have ongoing and planned programs in adaptive optics (AO) that require a detailed knowledge of the optical turbulence profile (OTP) over this observatory.

Optical turbulence in the atmosphere is a non-stationary process. Individual OTPs differ from one another in random way, making it difficult or even impossible to use raw data in the AO system studies. Instead, a *model OTP* is required that would summarize the main characteristics of turbulence at a given site in a form suitable for predictions of instrument performance. Such models have been developed in the past (Hufnagel 1974; Abahamid et al. 2004a). The OTP at CP has been characterized for the first time during the 1998 Gemini site campaign (Vernin et al. 1998) and a model OTP consisting of seven discrete layers has been derived from this study by Ellerbroek & Rigaut (2000) – hereafter ER2000. This model rapidly gained popularity in the AO community and has been used by many groups in their simulations.

The ER2000 model is insufficient in two respects. First, it does not address the variability of the OTP. Some researchers scaled this model to account for changing seeing conditions, keeping the same relative strength of layers. This does not correspond to the real situation where turbulence in the high and low atmosphere varies independently. Challenging science will be done under better-than-average conditions, hence AO system design and performance predictions must consider favorable OTPs along with median and bad ones.

Second, the ER2000 model was developed for the needs of classical and multiconjugate AO that is mostly affected by high-altitude turbulence. The model puts 65 per cent of turbulence in a single layer at zero altitude, the next layer being at 1.8 km. Such a coarse description of the ground layer (GL) is insufficient for predicting the performance of ground-layer AO (GLAO) systems designed for SOAR (Tokovinin et al. 2004) and under study for Gemini. Yet, the ER2000 model already has been used in GLAO studies (Chun 2003) because nothing else was available. In this paper we re-analyse the existing data complemented with new measurements to derive a more detailed *statistical* OTP model for CP with emphasis on the GL.

The standard geophysical division of the atmosphere into three zones – surface (or ground) layer, boundary layer and free atmosphere (FA) – is hardly applicable to night-time OTP at mountain observatories where interaction of air flow with the relief may extend to several kilometres above observatory. In the context of this paper, we consider the ground layer (GL) as a zone from the telescope (10–50 m) to some 500 m above the site. The zone above the GL is called FA. Similar approach has been taken by Abahamid et al. (2004a), except that they consider the GL to extend up to 1 km.

OTP is universally defined as the dependence of the refractive index structure constant C_n^2 on altitude h. Usually, h is given above sea level, but here h is counted above the site level, as this is more convenient for GLAO analysis. The C_n^2 is measured in $\mathrm{m}^{-2/3}$. Turbulence integrals $J = \int C_n^2(h)\,\mathrm{d}h$ over some altitude range are measured in $\mathrm{m}^{1/3}$. Astronomers usually express turbulence strength as 'seeing' ϵ [image full width at half-maximum (FWHM) size]. To be more

★E-mail: atokovinin@ctio.noao.edu (AT); tonyt@caltech.edu (TT)

specific, 'seeing' is the theoretical image size for Kolmogorov turbulence at $\lambda = 500$-nm wavelength at zenith (the atmospheric image quality is always better that ϵ because of the outer-scale effects). The seeing and Fried parameter r_0 are related to the turbulence integral J as

$$\epsilon = (J/6.8 \times 10^{-13})^{0.6} \text{ arcsec}, \quad (1)$$

$$r_0(\lambda)^{-5/3} = 0.423 J (2\pi/\lambda)^2. \quad (2)$$

Seeing or r_0 are not additive, hence we rather prefer to use the integrals J. Whenever the seeing values are quoted, they are equivalent to J in the sense of (1). The values with indices GL and FA refer to the ground layer and free atmosphere, respectively.

Previous OTP models were focused mostly on average or median profiles, e.g., Abahamid et al. (2004a). Yet, strong variability of the OTP is an essential property of turbulence that has to be taken into account for correct predictions of instrument performance. The variability of integrated quantities such as seeing or isoplanatic angle is not dramatic. For example, Racine (2005) shows in his compilation that the seeing distribution is close to log-normal, with quartiles-to-mean ratios of 0.8 and 1.2 (or 0.74 and 1.35 for turbulence integrals). However, turbulence intensity at any given altitude changes by *several orders of magnitude!* Thus, the average OTP is almost 10 times larger than the median OTP (Abahamid et al. 2004a). Both are practically featureless, as also noted by Racine (2005). But real OTPs are typically dominated by few strong layers. As a result, seeing and other atmospheric parameters are determined by these layers, not by the median or average OTPs, and the use of such OTPs for AO studies may be misleading.

We implement a new approach to OTP modeling: first, the data are sorted on some relevant parameter and then averaged separately in each group to reveal typical features. Using this method, we show that the shape of the OTP changes along with its integral. Turbulence in the FA occurs at lower altitudes when it becomes stronger, and the thickness of the GL increases with increasing GL integral. We select the groups to be representative of good conditions (best 25 per cent of nights), typical (or median) conditions and bad conditions (75 per cent of nights), according to some relevant parameter. The choice of ranking criterion is not unique, depending on the intended use of the model. Here, the models are ranked on turbulence conditions in the FA and are thus tailored to the needs of GLAO studies. Hopefully, this method will be applied to other sites and other data sets.

The previous OTP model for CP was based on only 45 balloon profiles. Here the statistics is greatly enhanced and the first substantial number of seeing measurements at CP is reported. However, there are some discrepancies between various data sets caused by real changes of the atmosphere and by instrumental biases. Our work clearly shows and discusses these differences, as well as the limitations of individual techniques such as SODAR. The model proposed here is by no means 'definitive', it is only an approximate synthesis of available data. Yet, the model responds to the needs of current AO projects and will serve until new significant data on the atmosphere at CP are obtained.

The equipment and data are discussed in Section 2. Then in Sections 3 and 4 we model the OTP in FA and in the ground layer. Section 5 discusses the results, the conclusions are given in Section 6.

2 EQUIPMENT AND DATA

New methods of OTP measurement are being developed nowadays, such as SLODAR (Wilson 2002) which is particulary suited for GL characterization. We do not intend a comprehensive review of these methods here, but rather present briefly the instruments used at CP and their data.

2.1 Balloons

Microthermal balloon soundings of the atmosphere over CP were conducted in 1998 in the framework of Gemini site characterization (Vernin et al. 1998; Avila et al. 2000). It consisted of four 1-week missions in 1998 that covered 40 nights distributed over all seasons. The equipment is described by Azouit & Vernin (2005). High vertical resolution (∼6 m) of the microthermal data makes them particularly suitable for modeling OTP near the ground. The balloons were launched from the summit of CP, close to the actual location of the Gemini-South telescope. A total of 49 flights are reported in tables 3.6 and 3.7 of Vernin et al. (1998), but only 43 contain useful data in the GL. Still, according to Abahamid et al. (2004a), this is the largest set of balloon profiles for any astronomical observatory. These instantaneous 'snapshots' of OTP show the typical conditions at CP but have low statistical significance, owing to the small number of profiles. Moreover, the first part of balloon trajectory is often distorted by local wind flows, leading to uncertain altitudes of the lowest data points.

The digital profiles were obtained from Gemini for the purpose of GLAO modeling. The C_n^2 values used here are the average from measurements with two microthermal baselines, 30 and 95 cm. Fig. 1 plots all profiles integrated in logarithmic altitude bins of the width 2. The scatter of points at low altitudes reaches three orders of magnitude, showing the difficulty of using this statistical sample for modeling.

2.2 MASS and DIMM

Low-resolution OTPs have been measured at CP in 2003 January using Multi-Aperture Scintillation Sensor (MASS) (Kornilov et al. 2003). The principle of this instrument and its limitations are described by Tokovinin et al. (2003b). Its vertical resolution is only half of altitude, turbulence below 0.5 km is not sensed. The total seeing has been measured simultaneously with the Differential Image Motion Monitor (DIMM). The same combination of instruments has been used previously to study the OTP statistics at a nearby summit of Cerro Tololo (CT) (Tokovinin, Baumont & Vasquez 2003a), we

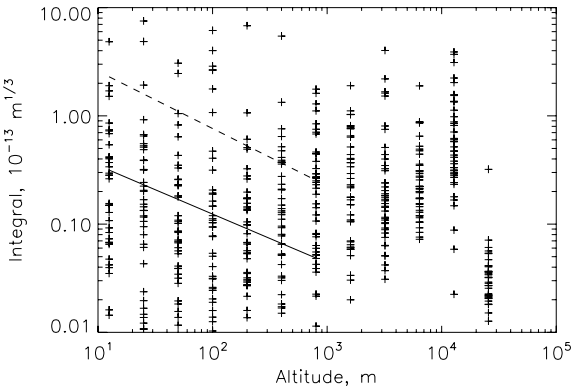

Figure 1. Individual OTPs from CP-1998 balloon data. The integrals in logarithmic altitude bins of the width 2 are plotted. The bin centres are at 12.5, 25, 50 m, . . . , 25.6 km. Power-law models of Abahamid et al. (2004a) for the first kilometre are overplotted (full line – median profile, dashed line – mean profile).

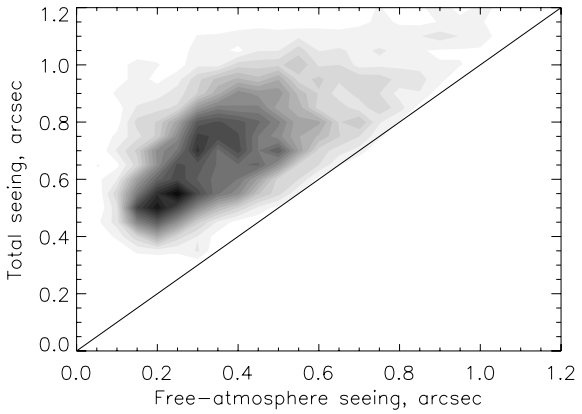

Figure 2. Comparison of simultaneous measurements of seeing in the FA with MASS and total seeing with DIMM (CP2005 data). The density of points is displayed in gray-scale.

refer the reader to that paper for further details. The only difference is that here MASS data were slightly corrected for 'overshoots' under strong scintillation, where the original data processing based on the weak-scintillation theory overestimated turbulence strength.

The 2003 CP campaign covered 23 nights (January 8–18 and 22–31). A total of 4234 OTPs with 1-min temporal resolution was measured. When the seeing was dominated by high layers, there was a very good mutual agreement between MASS and DIMM. This inspires confidence in the estimates of the GL seeing obtained by subtracting the integrals from these instruments. Unfortunately, the DIMM was installed only at 1.5 m above ground and hence was strongly affected by surface-layer turbulence, overestimating the $J_{\rm GL}$.

In 2004 a combined MASS–DIMM seeing monitor has been installed at CP in a 6-m high tower. Here the DIMM and MASS channels are fed simultaneously by splitting the light in the exit pupil of a 25-cm Meade telescope. Unfortunately, this system has yet not been fully operational during our SODAR run in 2004. We extracted the MASS–DIMM data for the period from 2004 December 1 to 2005 April 15 (6619 profiles, called CP2005 hereafter). Again, a good match between MASS and DIMM is found (Fig. 2). Two physically distinct MASS and DIMM instrument sets produced very concordant results in 2003 and 2005. The CP2005 data set provides the first reliable measurement of total seeing at CP, the 25, 50 and 75 per cent levels of the distribution being 0.63, 0.77 and 0.91 arcsec. Abahamid et al. (2004b) estimated the median seeing at CP as 0.75 arcsec from the balloon data. The CP2005 data show a median contribution of the GL to the total integral to be 61 per cent, in line with the 1998 balloon results and the ER2000 model.

2.3 SODAR

Acoustic sounders – SODARs – have been used on many occasions to study microthermal fluctuations in the atmospheric boundary layer at astronomical sites, e.g. at Maidanak (Gur'yanov et al. 1992) and Dome C (Lawrence et al. 2004). The results obtained so far were often considered controversial because absolute calibration of SODAR is notoriously difficult and uncertain. On the other hand, SODAR gives rich information on the location and evolution of turbulence in the first few hundred meters, unsurpassed by any other technique available so far.

The SODAR (model XFAS from Scintec[1]) has been deployed on CP not far from the site monitor tower, from 2004 October 30 to November 16. The issue addressed by this campaign is the thickness of the GL at CP, it does not require absolute SODAR calibration. Three directions of acoustic beam were used: vertical, south and east. In this way we tried to avoid acoustic echoes from the Gemini dome (to the west) and seeing tower (to the north). The software from Scintec assured automatic control of SODAR operation and on-line data reduction. The SODAR was programmed to start operation at 20:30 local time (23:30 UT) every evening and worked continuously until 7:30 local (10:30 UT). Each profile is obtained after 20-min accumulation of data. The vertical resolution of SODAR is 20 m, the lowest bin is at 40 m and the highest one is at 800 m above ground. The first 40 m are not sensed.

Original on-line data processing revealed that temperature fluctuations dropped rapidly in the first 100 m and then slowly increased again at altitudes above 400 m. This behaviour is characteristic of acoustic noise, according to prior experience with this SODAR. The likely source of this noise (which was variable from one night to another) is wind. The SODAR data was then reprocessed, filtering out the noise as much as possible and applying the calibration to convert the back-scattered signal to the temperature structure constant C_T^2. The calibration process, which is completely described by Travouillon et al. (in preparation), involved daytime measurements of the OTP. As stated by the Monin–Obukhov similarity, under unstable atmospheric conditions the C_T^2 can be related to the turbulent heat flux H:

$$C_T^2(h) = \frac{2.8H^{4/3}}{(c_p\rho h)^{4/3}(g/T)^{2/3}}, \tag{3}$$

where c_p is the heat capacity of air, ρ its density, g is the gravitational constant and T the temperature. Several calibration profiles have been obtained while simultaneously measuring the solar heat flux, assumed to be equal to H. The calibration curves were then averaged and used on the night-time profiles. The conversion between C_T^2 and C_n^2 is carried out using the local weather station measurement of the temperature T [K] and pressure P [mbar]:

$$C_n^2(h) = \left(79 \times 10^{-6}\frac{P}{T^2}\right)^2 C_T^2(h). \tag{4}$$

As only the ground temperature is available, we extrapolate upwards using the standard lapse rate of 6.5 K km^{-1}. Humidity is taken into account as explained by Travouillon et al. (in preparation). During the campaign, high humidity was encountered after November 12/13. Moreover, some precipitation occurred at CP on November 12/13, showing up in very atypical SODAR profiles (strong echo from 40-m level, nothing above). The night of November 12/13 was excluded from further analysis. This leaves 495 SODAR profiles covering a total of 168 h. The half-tone representations of the data for two typical nights are shown in Fig. 3. Each plot is normalized arbitrarily.

The paucity of simultaneous MASS–DIMM data precluded direct comparison with SODAR during the CP campaign. However, such comparison has been done shortly after, while testing the portable SLODAR at CT (Wilson et al., in preparation). The results are shown in Fig. 4 and prove that the SODAR calibration was correct. The best-fit line (curve in log–log coordinates) shows that MASS–DIMM GL integrals have a constant offset, corresponding to turbulence below 40 m not sensed by SODAR. This difference is even stronger at

[1] http://www.scintec.com

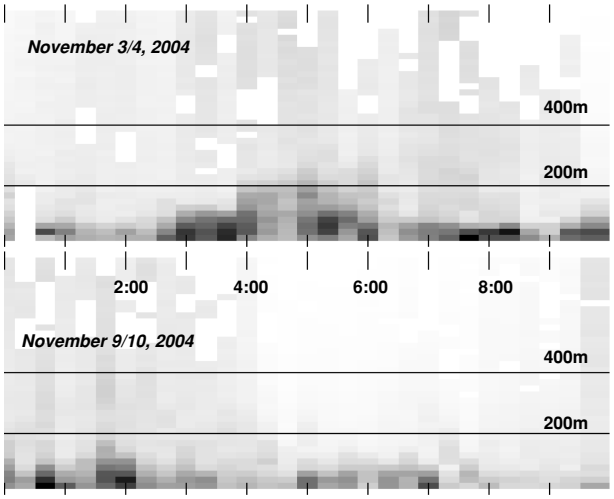

Figure 3. SODAR profiles on November 3/4 and 9/10, 2004. Turbulence intensity is displayed with a negative scaling and square-root stretch. The horizontal lines mark the 200 m and 400 m levels, the vertical ticks mark UT hours from 0 to 10 h.

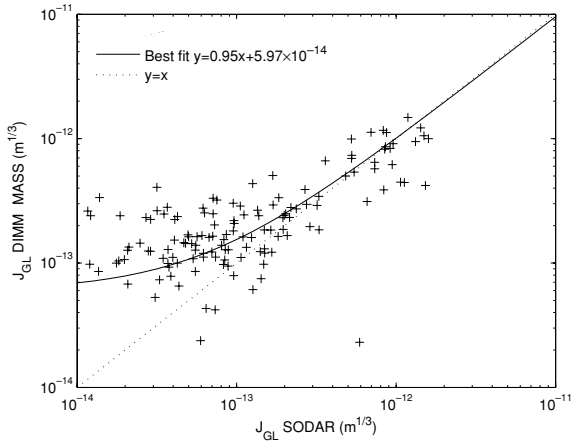

Figure 4. The GL integrals as measured simultaneously by SODAR and MASS–DIMM at CT during SLODAR campaign (2004 November–December), with a linear regression line.

CP, suggesting a thinner ground layer than at CT. However, when the CP–SODAR data are properly modeled and extrapolated, we recover a good agreement with MASS–DIMM.

Apart from the offset, we note a large (∼2 times) scatter of points around the best-fit line. It is too big to be explained by statistical errors of these 20-min averages. We attribute this scatter to a large variability of GL turbulence (the volumes sampled by MASS–DIMM and SODAR do not coincide spatially) and to the different physical principles of these instruments.

3 MODEL OF FREE ATMOSPHERE

First of all, we want to know the relative strength of turbulence in FA and GL and the limits of its variability. Low-resolution OTPs from MASS–DIMM are particularly useful for this purpose. Large data sets have been acquired both at CP and at the nearby mountain CT (Tokovinin et al. 2003a). The FA integrals measured at CT should be representative of CP, given the proximity of the sites.

The available statistical data are gathered in Table 1 that gives the percentiles of the cumulative distributions. For each data set we give the number of nights $N_{\rm night}$ and the number of individual OTPs $N_{\rm OTP}$ that contributed to the statistics. It can be inferred that the distributions of the integrals resemble log-normal ones, with the ratio of 25 and 75 per cent quartiles to the median being close to 1.8^{-1} and 1.8, respectively. Please, note that the quartiles of the total integral $J_{\rm TOT} = J_{\rm GL} + J_{\rm FA}$ cannot be obtained as sums of the correponding quartiles in Table 1. Indeed, the GL and FA being independent (see below), a combination of the best 25 per cent conditions in both FA and GL corresponds to the $0.25^2 = 0.06$ fraction of nights, not to 0.25.

The adopted boundary between GL and FA is slightly different for these data sets. SCIDAR measurements at CT consider FA above 1 km (that corresponds to 600 m above CP because CT is 400 m lower), as reported in fig. 3.33 of Vernin et al. (1998) ('dome processing'). The 1998 balloon profiles were integrated between 8 and 600 m for GL and above 600 m for FA. The MASS–DIMM data for CT (Tokovinin, Baumont & Vasquez 2003a) and CP correspond to FA integrals with a peculiar 'weighting function' (MASS sensitivity) that grows linearly from 0 to 1 on the interval from 250 to 500 m, then stays constant. The GL integrals are obtained by subtracting the FA integrals from the total integral $J_{\rm TOT}$ measured with DIMM, hence the MASS–DIMM GL weight is just the inverse, being 1 up to ∼250 m and then falling to 0 at 500 m. We note that this disparity of the definitions of the boundary between FA and GL has only minor effect on the integrals because turbulence near this boundary is usually weak, of the order 10^{-16} m$^{-2/3}$. Thus, a boundary uncertainty of 200 m would change the GL and FA integrals by only 2×10^{-14} m$^{1/3}$. The lowest GL limit is set by the altitude of the DIMM (6 m in 2005, 1.5 m in 2003).

There is a resonably good agreement of FA integrals between these disparate data sets, the difference being explainable by the natural variation of site properties. For example, the 2002 CT data cover a winter period when the turbulence is stronger than in summer. The FA parameters measured by MASS are gathered in Table 2. It is evident from Fig. 2 that $\epsilon_{\rm FA}$ is *never* better than 0.1 arcsec! This conclusion has been already evident from the work of Vernin et al. (1998). Better $\epsilon_{\rm FA}$ has been seen only at Dome C (Lawrence

Table 1. Levels of the cumulative distributions of turbulence integrals $J_{\rm GL}$ and $J_{\rm FA}$, in 10^{-13} m$^{1/3}$.

Ground layer			Free atmosphere			$N_{\rm night}$	$N_{\rm OTP}$	Site, year, instrument
25 per cent	50 per cent	75 per cent	25 per cent	50 per cent	75 per cent			
0.77	1.80	4.49	1.18	2.14	5.08	22	6900	CT, 1998, SCIDAR
0.54	1.14	2.85	0.95	1.73	3.14	40	43	CP, 1998, Balloons
1.93	3.40	4.98	1.35	2.51	4.88	58	28000	CT, 2002, MASS–DIMM
(3.84)	(5.41)	(7.37)	0.87	1.44	2.75	21	4234	CP, 2003, MASS–DIMM
(0.22)	(0.48)	(1.11)	–	–	–	16	495	CP, 2004, SODAR
1.52	2.37	3.51	0.85	1.52	2.63	69	6619	CP, 2005, MASS–DIMM
2.2	2.7	3.3	0.85	1.5	2.5	–	–	CP model

Table 2. Levels of the cumulative distributions of seeing ϵ_{FA} and isoplanatic angle θ_0 from MASS data.

ϵ_{FA} (arcsec)			θ_0 (arcsec)			Year
25 per cent	50 per cent	75 per cent	25 per cent	50 per cent	75 per cent	
0.38	0.55	0.82	2.36	1.80	1.30	2002
0.29	0.39	0.58	2.54	2.16	1.87	2003
0.29	0.41	0.56	2.82	2.35	1.90	2005
0.29	0.40	0.55	2.58	2.22	2.04	CP model

et al. 2004). However, periods of very good and stable conditions in the FA with $\epsilon_{FA} \sim 0.2$ arcsec do occur regularly at CP and CT (see the clump in Fig. 2). The longest such period in June 2002 lasted for four nights (Tokovinin et al. 2003a). *A judicious use of these periods for doing challenging AO science will be very rewarding.*

The individual OTPs show a wide variety of shapes. Fitting a model to these data is a difficult and ambiguous task. Average OTP always overestimates the turbulence, median OTP underestimates it. Ellerbroek & Rigaut (2000) fitted seven discrete layers to the *median* balloon OTP in such way as to match all moments up to some order. Here we take the CP2005 MASS data, sort them on J_{FA} and average the OTPs in groups around the quantiles of this distribution. Thus, a 'good' OTP corresponds to the J_{FA} values comprised between 20 and 30 per cent and is representative of best 25 per cent conditions in the FA. Similarly, the typical OTP is averaged between 45 and 55 per cent, and the bad OTP between 70 and 80 per cent. Each group contains some 660 OTPs. The resulting average OTPs are plotted in Fig. 5. The CP2003 data were processed in the same way and show a similar pattern. Interestingly, the turbulence in the highest 16-km layer is almost constant, causing a seeing of 0.15 arcsec. The variations of J_{FA} are mostly caused by appearance of turbulence at lower altitudes.

Guided by these data, we propose in Table 3 a model of FA for good, typical and bad conditions. The corresponding GL intensities J_{GL} are also given, adjusted to fit the cumulative distribution of the total integral, rather than the distribution of J_{GL} given in Table 1. Thus, the model in Table 3 is representative of the 25 per cent best, median and 75 per cent of nights *ranked in terms of the FA seeing*, but it does not match the OTP quartiles in each layer separately, as evidenced also by comparison with Fig. 5. We show below that these three models adequately describe the performance of a GLAO system, and for this purpose we can replace the individual measured OTPs.

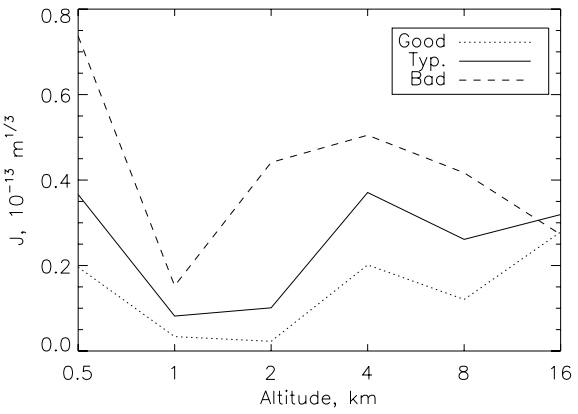

Figure 5. OTP in the FA according to the MASS 2005 data averaged in groups. Good corresponds to the best 25 per cent conditions in the FA, typical – to the median FA conditions, and bad – to 75 per cent of nights.

Table 3. Model of the CP atmosphere (integrals J in 10^{-13} $m^{1/3}$). The seven-layer model of ER2000 is given for comparison.

h (km)	0	0.5	1	2	4	8	16
Good	2.2	0.2	0.03	0.02	0.2	0.15	0.25
Typical	2.7	0.4	0.1	0.1	0.4	0.2	0.3
Bad	3.3	0.7	0.2	0.4	0.6	0.3	0.3
h (km)	0	1.8	3.3	5.8	7.4	13.1	15.8
ER2000	1.93	0.23	0.36	0.10	0.07	0.24	0.04

The integral parameters of these models – seeing and isoplanatic angle – are given in Table 2, to be compared to the actual distributions. The ER2000 model is given for comparison in Table 3. It corresponds to good, rather than median, conditions at CP, and predicts a seeing of 0.61 arcsec, $\epsilon_{FA} = 0.33$ arcsec and $\theta_0 = 2.74$ arcsec. The reason can be traced to the fact that a median OTP always underestimates the median conditions.

A loose anticorrelation between J_{FA} and θ_0 is noted in the scatter plots of the CP2005 and CP2003 data: as turbulence gets stronger, θ_0 decreases as $\theta_0 \approx 1'' \, (J_{FA}/12^{-12})^{-0.4}$. It is possible to represent the FA by a single layer with changing altitude and strength that would fit both J_{FA} and θ_0. As turbulence increases, this layer gets lower, $h \propto J_{FA}^{-0.2}$. However, the merit and usefulness of such a single-layer FA model are doubtful because it does not lead to good predictions for GLAO.

4 MODEL OF THE GROUND LAYER

The integrals J_{GL} given in Table 1 show a much larger scatter between different techniques compared to J_{FA}. Part of this discrepancy is due to the poor definition of this parameter – its strong dependence on the lower altitude limit or location on the site. For example, the MASS–DIMM measurements in 2003 overestimate J_{GL} owing to the low (1.5 m) DIMM altitude, while SORDAR integrals are too low because they miss everything below 40 m.

Now we address the difficult problem of modeling the thickness of the GL. The best set of high-resolution OTPs for CP comes from the 1998 balloon campaign. The range of C_n^2 variation in individual OTPs is enormous (Fig. 1). Averaging these OTPs will lead to a dominating contribution of strong turbulence, hence the average OTP is *not* a good statistical characteristic. We subdivided the set of 43 OTPs into three groups: 11 good, 20 typical and 12 bad. Different criteria for splitting into groups were tried (e.g., total seeing, GL seeing, GL thickness), with similar results. The final criterion is a product of GL seeing and effective GL thickness. The groups correspond roughly to 25 per cent best, 50 per cent typical and 25 per cent worst conditions of GL turbulence.

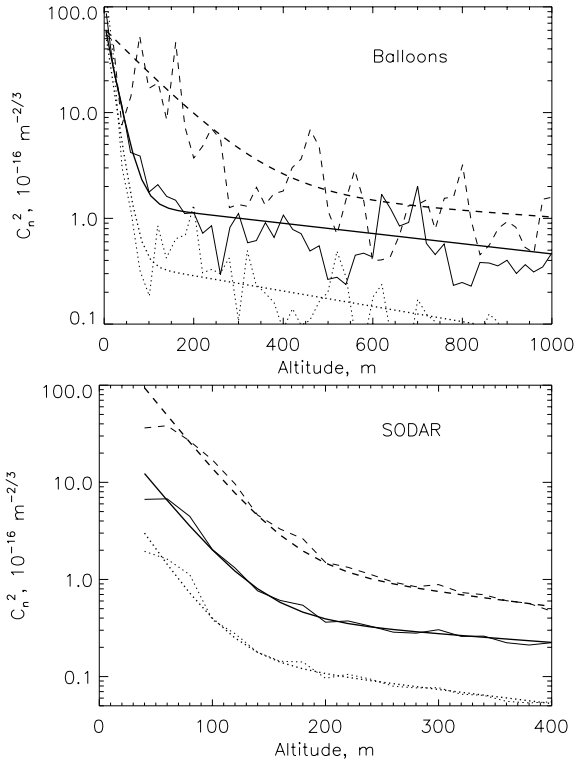

Figure 6. The OTPs averaged in 3 groups (good – dotted line, median – full line, bad – dashed line) are compared to their analytic models (5) plotted in thick lines for the balloon 1998 data (top) and SODAR 2004 data (bottom).

The average OTP in each group was roughly modeled by a combination of two exponents,

$$C_n^2(h) = A\ \exp(-h/h_0) + B\ \exp(-h/h_1). \quad (5)$$

The average OTPs and corresponding models are plotted in Fig. 6. Even the average OTPs are very irregular – a consequence of small statistics and large turbulence variability. Hence, it was essential to complement the balloon data with SODAR

The SODAR integrals of the OTP from 40 to 500 m are given in Table 1. Clearly, they seem to be systematically smaller compared to other GL data. Compared to balloons, the altitude range of SODAR data is more restricted. We also noted that the SODAR OTPs start to grow at altitudes above 400 m, likely because of the remaining acoustic noise. Thus, we model the OTP only in the first 40–400 m range by two exponents (equation 5).

The data were also split into three groups according to the GL seeing: good (first quartile), typical (50 per cent profiles around the median) and bad (last quartile). The parameters of the models roughly fitted to the average OTP in each group are gathered in Table 4, the average OTPs and models are plotted in Fig. 6. Note that the average integrals $J_{\rm GL}$ are systematically larger than the quantiles of the cumulative distributions derived from the same data (Table 1). This happens because the models are fitted to the average OTP in each group, average is always larger than median.

Despite very different measurement techniques, altitude range and analysis method, there is a broad agreement on the characteristics of 'typical' profiles. Strong turbulence near the ground decays with a 1/*e* scale height of 20 m (balloons) or 30 m (SODAR) and produces a seeing around 0.5 arcsec. The larger scale height given by SODAR is explained by its lower vertical resolution that broadens the OTP. On the other hand, the first few metres of the balloon

Table 4. GL models derived from SODAR and balloons. N is the number of profiles in each group. The parameters A and B are in units of 10^{-16} m$^{-2/3}$, h_0 and h_1 in metres, the integral $J_{\rm GL}$ (from 6 to 500 m) in 10^{-13} m$^{1/3}$.

Group	N	A	h_0	B	h_1	$J_{\rm GL}$
SODAR						
Good	125	12	25	0.20	300	0.31
Typical	247	45	30	0.5	500	1.26
Bad	123	350	30	2.0	300	9.07
Balloons						
Good	11	70	15	0.4	700	0.84
Typical	20	70	20	1.4	900	1.56
Bad	12	60	100	2.0	1500	6.44

OTPs are unreliable, as noted above. At altitudes above 200 m a typical OTP levels at $\sim 10^{-16}$ m$^{-2/3}$ and continues to decay more slowly. When the GL turbulence is weak, it concentrates strongly to the ground according to balloons. This part of the OTP is not sensed by SODAR, hence its results under good conditions are suspect. A large difference between the integrals of the SODAR *models* and the raw integrals $J_{\rm GL}$ in Table 1 is explained by the extrapolation of models to low altitudes and by the bias between averaged (models) and median (raw data) quantities mentioned above. The first point of the average SODAR profiles is below exponential models, hinting at possible flattening of the profiles close to the ground.

Abahamid et al. (2004a) suggested a power-law model of the OTP in the first kilometre above ground,

$$C_n^2(h) = C\ (h/1{\rm m})^{-p}, \quad (6)$$

where the exponent p is close to 1.5 and the coefficient C is 1.39×10^{-13} m$^{-2/3}$ for the median OTP and 1.24×10^{-12} m$^{-2/3}$ for the mean OTP. The integrals of this model depend sensitively on the lower limit, reflecting the above-mentioned ill definition of $J_{\rm GL}$. Integrating (6) from 6 to 500 m leads to $J_{\rm GL} = 1.0 \times 10^{-13}$ for the median OTP and 9.0×10^{-13} for the mean OTP. We tried to fit (6) with $p = 1.5$ to our data and found that the measured C_n^2 profiles decay with altitude faster than this model.

Our data are well matched by integrable exponential models, preferred for this reason over the power law (6). Racine (2005) also uses a negative exponent to describe turbulence in the surface layer. However, neither of these models can be used directly in modern software for AO simulation that requires a representation of the OTP by discrete thin layers. The GL should be modeled as one or several layers, depending on the sensitivity of the particular AO system to its thickness. For example, in case of GLAO Tokovinin (2004) shows that all turbulence within $H_{\rm min} = d/(2\theta)$ from the conjugation height of the deformable mirror can be safely modeled by a single layer (d is the actuator spacing, θ is the radius of the corrected field-of-view). Assuming, for example, $d = 0.5$ m and $\theta = 1'$, we estimate $H_{\rm min} = 0.9$ km, hence a one-layer GL model is sufficient. In case when a much wider field is corrected, a GL model with more layers is needed.

It is interesting to study the dependence of GL turbulence on local meteorological parameters. The meteorological data (pressure, wind speed and direction, relative humidity and temperature) were extracted from the regular meteo services of Gemini and SOAR. These data were matched in time with SODAR and MASS–DIMM (CP2005) and analysed jointly for possible correlations. It appears that $J_{\rm GL}$ is independent of the wind speed according to MASS–DIMM but increases with wind according to SODAR (Fig. 7). This behaviour can be explained if the thickness of the GL increases

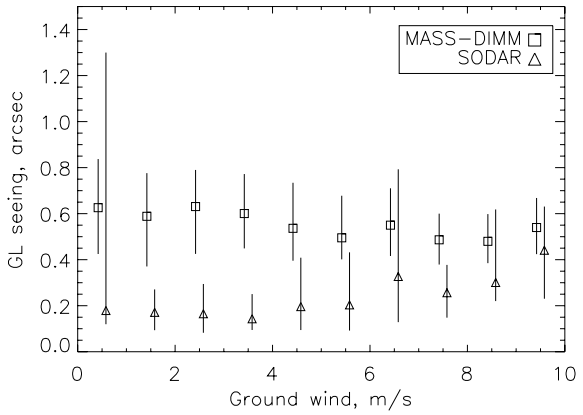

Figure 7. Correlation of GL seeing with the ground wind speed according to SODAR and MASS–DIMM (CP2005). The data are binned in 1 m s^{-1} intervals, with median values in each interval plotted as symbols and the 68 per cent of values around median ('$\pm 1\sigma$') indicated by bars.

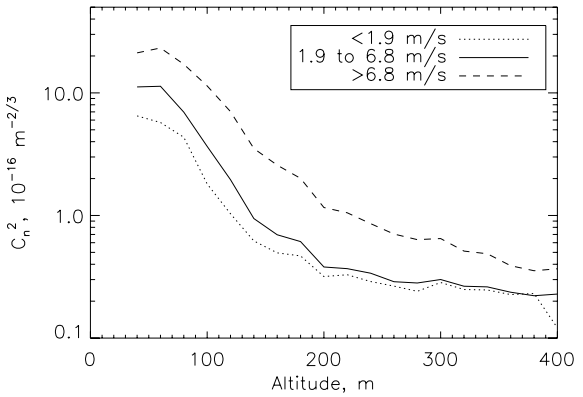

Figure 8. SODAR profiles averaged in groups according to the ground wind speed.

with increasing wind speed (Fig. 8). A large difference between the instruments is caused by turbulence concentration below 40 m. The relationship between GL turbulence and wind speed has been studied at some other sites (Ehgamberdiev et al. 2000; Travouillon et al. 2003), and no correlation of GL seeing with wind was found [such a correlation exists at CT (Tokovinin et al. 2003a)]. The diurnal dependence of GL seeing (not plotted) shows a turbulence decay in the first 2 h after sunset. Moreover, the probability of bad GL seeing seems to increase after local midnight, as might be guessed from the episodes of strong turbulence seen in Fig. 3.

5 DISCUSSION

The data presented in this paper lead to representative models of the OTP at CP for different observing conditions, ranked on either FA or GL seeing: good (25 per cent of time), bad (75 per cent) and typical (median). It is important to note that there is no correlation between the GL and FA, as shown in Fig. 9. The absence of correlation can be confirmed with other data sets for CP discussed here, no such correlation was found at Mauna Kea (Tokovinin et al. 2005). Hence, the parameters of the OTP model should be selected independently for GL and FA and then combined together.

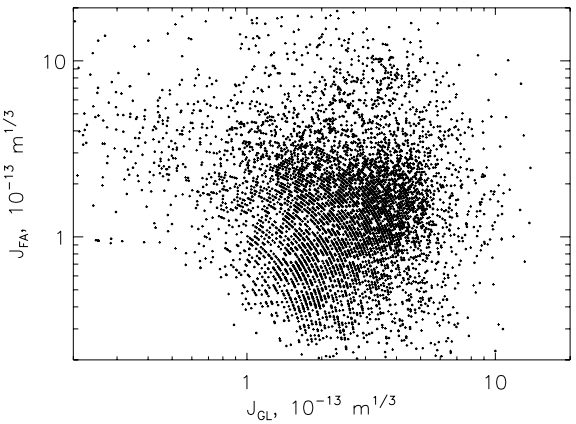

Figure 9. Lack of correlation between turbulent integrals in the FA and ground layer (CP2005 data).

Mutual independence of GL and FA explains why the conditions of very good seeing are rare at any site. The periods of calm FA happen regularly, but they need to coincide with calm GL to produce exceptional seeing. Similarly, we take note that either FA or GL can spoil the seeing to above 1 arcsec, the probabilities of these events being additive. The distributions of the integrals in GL and FA resemble logarithmically-normal ones, with half of values lying within 1.8 times of the median. The distribution of the total seeing also seems to be log-normal, with quartile ratio of 0.8/1.2 as at other sites (Racine 2005).

As an example of the application of our OTP model, we show in Fig. 10 a statistical prediction of the FWHM resolution at three wavelengths after partial correction of turbulence by the SOAR Adaptive Module (SAM) (Tokovinin et al. 2004). This GLAO system will correct about 45 Zernike modes using a Rayleigh laser guide star at 10 km from the telescope and two tip-tilt guide stars outside the science field of 3 arcmin diameter. The GL is corrected preferentially because of the intentionally low beacon altitude. The on-axis FWHM image size in SAM has been computed by the method of Tokovinin (2004) for observations at zenith, for each of 6619 individual OTPs (CP2005 data). Its cumulative distributions (at three wavelengths) are plotted in Fig. 10. The same method have been applied to the model (instead of individual) OTPs, the results are shown as squares. The correspondence between GLAO predictions from

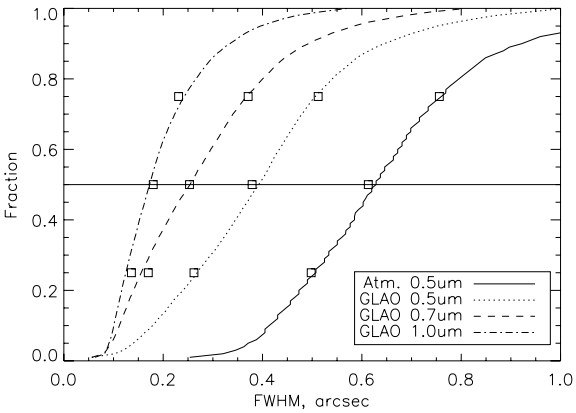

Figure 10. Cumulative distributions of the FWHM image size at three wavelengths (0.5, 0.7 and 1.0 μm) predicted for the SAM AO system, according to the CP05 data. The corresponding values for our three OTP models are overplotted by squares.

our OTP models and the distributions obtained from real profiles is not exact, but reasonably good. Thus, we can replace thousands of individual OTPs by three representative models for the purpose of GLAO studies. Note that the uncorrected FWHM at 0.5 μm is better than the seeing because a finite outer scale $L_0 = 25$ m was assumed in the calculation.

6 CONCLUSIONS

The main conclusion of this paper is that the OTP at CP is highly variable. Using a single OTP model may be misleading, hence we propose here a statistical model that describes good, typical, and bad conditions separately. The OTP in the FA is well constrained by the available data, all methods give coherent results. On the other hand, the GL model is still preliminary. Turbulence in GL and FA is generated by different mechanisms, the resulting OTP is a combination of these two independent components.

Further studies will bring more information on the connection between OTP and meteorological parameters, possibly involving computational fluid-dynamics simulations to understand the contribution of the local topography. The data hint that the FA seeing is correlated with the speed of the high-altitude wind (Tokovinin et al. 2003a), while the GL seeing may depend on the local wind. Further understanding of these relations will eventually lead to *predicting* the OTP.

ACKNOWLEDGMENTS

The contribution of CTIO engineers J. Seguel, E. Bustos, D. Walker and J. Vasquez has been essential in collecting the data for this study. We thank Gemini staff for providing the archival data of the 1998 campaign and for enthusiastically supporting the 2004 SODAR campaign at CP. Part of this work has been done in the framework of the GLAO conceptual study for Gemini. The SOAR director S. Heathcote and SOAR staff contributed significantly by organizing the 2003 MASS–DIMM campaign and by supporting the construction of the CP site monitor – a joint project between Gemini and SOAR.

REFERENCES

Abahamid A., Jabiri A., Vernin J., Benkhaldoun Z., Azouit M., Agabi A., 2004a, A&A, 416, 1193
Abahamid A., Vernin J., Benkhaldoun Z., Jabiri A., Azouit M., Agabi A., 2004b, A&A, 422, 1123
Avila R., Vernin J., Chun M. R., Sánchez L. J., 2000, Proc. SPIE, 4007, 721
Azouit M., Vernin J., 2005, PASP, 117, 563
Chun M., 2003, Proc. SPIE, 4839, 94
Ehgamberdiev S. A., Baijumanov A. K., Ilyasov S. P., Sarazin M., Tillayev Y. A., Tokovinin A. A., Ziad A., 2000, A&AS, 145, 293
Ellerbroek B. L., Rigaut F. J., 2000, Proc. SPIE, 4007, 1088 (ER2000)
Gur'yanov A. E., Kallistratova M. A., Kutyrev A. S., Petenko I. V., Scheglov P. V., Tokovinin A. A., 1992, A&A, 262, 373
Hufnagel R. E., 1974, in Optical Propagation Through Turbulence, OSA Technical Digest Series. OSA, Washington, DC, p. WA1-1
Kornilov V., Tokovinin A., Voziakova O., Zaitsev A., Shatsky N., Potanin S., Sarazin M., 2003, Proc. SPIE, 4839, 837
Lawrence J. S., Ashley M. C. B., Tokovinin A., Travouillon T., 2004, Nat, 431, 278
Racine R., 2005, PASP, 117, 401
Tokovinin A., 2004, PASP, 116, 941
Tokovinin A., Baumont S., Vasquez J., 2003a, MNRAS, 340, 52
Tokovinin A., Kornilov V., Shatsky N., Voziakova O., 2003b, MNRAS, 343, 891
Tokovinin A., Thomas S., Gregory B., van der Bliek N., Schurter P., Cantarutti R., Mondaca E., 2004, Proc. SPIE, 5490, 870
Tokovinin A., Vernin J., Ziad A., Chun M., 2005, PASP, 117, 395
Travouillon T., Ashley M. C. B., Burton M. G., Storey J. W. V., Loewenstein R. F., 2003, A&A, 400, 1163
Vernin J. et al., 1998, Gemini Site Testing Campaign, Cerro Pachón and Cerro Tololo. Gemini RPT-AO-G0094
Wilson R. W., 2002, MNRAS, 337, 103

This paper has been typeset from a TEX/LATEX file prepared by the author.